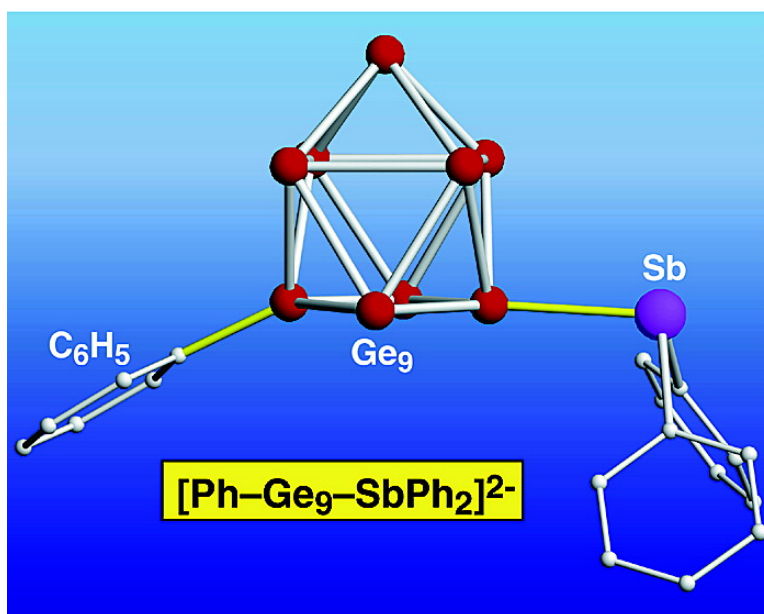


Derivatization of Deltahedral Zintl Ions by Nucleophilic Addition: $[\text{Ph-Ge-SbPh}]$ and $[\text{PhSb-Ge-Ge-SbPh}]$

Angel Ugrinov, and Slavi C. Sevov

J. Am. Chem. Soc., **2003**, 125 (46), 14059-14064 • DOI: 10.1021/ja037007b • Publication Date (Web): 25 October 2003

Downloaded from <http://pubs.acs.org> on March 30, 2009



More About This Article

Additional resources and features associated with this article are available within the HTML version:

- Supporting Information
- Links to the 10 articles that cite this article, as of the time of this article download
- Access to high resolution figures
- Links to articles and content related to this article
- Copyright permission to reproduce figures and/or text from this article

[View the Full Text HTML](#)



ACS Publications
 High quality. High impact.

Derivatization of Deltahedral Zintl Ions by Nucleophilic Addition: $[\text{Ph-Ge}_9\text{-SbPh}_2]^{2-}$ and $[\text{Ph}_2\text{Sb-Ge}_9\text{-Ge}_9\text{-SbPh}_2]^{4-}$

Angel Ugrinov and Slavi C. Sevov*

Contribution from the Department of Chemistry and Biochemistry, University of Notre Dame, Notre Dame, Indiana 46556

Received July 1, 2003; E-mail: ssevov@nd.edu

Abstract: The type of the reactions of addition of exo-bonded groups to deltahedral Zintl ions such as Ge_9^{n-} has been established as addition of anionic nucleophiles. Various nucleophiles such as Ph_2Bi^- , Ph_2Sb^- , Ph^- interact with the relatively low-lying LUMO of Ge_9^{2-} and/or the half filled HOMO of Ge_9^{3-} and bond to the clusters. The title anions, characterized in their (K-crypt) salts where *crypt* = 4,7,13,16,21,24-hexaoxa-1,10-diazabicyclo-[8.8.8]-hexacosane, and the previously characterized $[\text{Ph}_2\text{Sb-Ge}_9\text{-SbPh}_2]^{2-}$ are made by a reaction of K_4Ge_9 with SbPh_3 in ethylenediamine. $[\text{Ph-Ge}_9\text{-SbPh}_2]^{2-}$ is the first organically functionalized deltahedral Zintl ion, i.e., a deltahedral ion with a direct carbon-cluster covalent bond, that can exist without the substituents as well. The Ge_9 clusters resemble tricapped trigonal prisms with one elongated edge (one of the three edges parallel to the pseudo 3-fold axis). The two substituents are always bonded to the vertices of such an elongated edge. The same is true for the intercluster bond in $[\text{Ph}_2\text{Sb-Ge}_9\text{-Ge}_9\text{-SbPh}_2]^{4-}$.

Introduction

Zintl ions are polyatomic anions of the heavier main-group elements that can be stabilized in liquid ammonia or ethylenediamine and can be eventually crystallized from such solutions with appropriate counterions. A special group of such ions are the deltahedral Zintl ions of the heavier members in the carbon group, Ge, Sn, and Pb.¹ These are five- and nine-atom cage-like clusters with triangular faces and delocalized bonding as in the deltahedral boranes. The reactivity of these species, expected to be different from Zintl ions with normal 2-center-2-electron bonds, has not been sufficiently studied. Actually, until recently, the clusters were assumed to be so highly reduced that any attempt for oxidation was expected to destroy them. Thus, all studies of their chemistry were confined to Lewis acid-base reactions where the clusters were used as ligands to coordinate to transition metals via their lone pairs of electrons.² The first breakthrough in the redox chemistry of these species was the successful "oxidative" coupling of nine-atom germanium clusters into dimers of $[\text{Ge}_9\text{-Ge}_9]^{6-}$.³ This was quickly followed by the synthesis of a chain of clusters $^{\infty}[-(\text{Ge}_9^{2-})-]$,⁴ as well as smaller oligomers such as trimers and tetramers, $[\text{Ge}_9\text{=Ge}_9\text{=Ge}_9]^{6-}$ and $[\text{Ge}_9\text{=Ge}_9\text{=Ge}_9\text{=Ge}_9]^{8-}$, respectively.^{5,6} These results indicated that it should be possible

to covalently bond various groups to the clusters and synthesize the ultimate functionalized clusters. Reported recently was the first such derivatized deltahedral cluster $[\text{Ph}_2\text{Sb-Ge}_9\text{-SbPh}_2]^{2-}$ (**1**) made by a reaction of ethylenediamine solution of K_4Ge_9 with SbPh_3 .⁷ Here, we report the structures of two more products of the same reaction, the first organically functionalized deltahedral Zintl ion, $[\text{Ph-Ge}_9\text{-SbPh}_2]^{2-}$ (**2**), and a dimer of clusters functionalized with two diphenylantimony groups, $[\text{Ph}_2\text{Sb-Ge}_9\text{-Ge}_9\text{-SbPh}_2]^{4-}$ (**3**). Discussed at length is also the probable course of the reactions of addition to the clusters. It is determined that they are nucleophilic addition reactions where an anionic nucleophile Nu^- interacts with an empty or half-filled orbital of the cluster and forms an exo-bond.

Experimental Section

Synthesis. All manipulations were performed inside a nitrogen-filled glovebox with moisture level below 1 ppm. A precursor of nominal composition K_4Ge_9 was synthesized by heating (900 °C, 2 days) a stoichiometric mixture of the elements in niobium containers (arc-welded in Ar at low pressure) enclosed in quartz ampules under vacuum. Ethylenediamine solutions of this precursor were reacted with SbPh_3 in various molar ratios and at different temperatures. Nevertheless, these different conditions did not seem to affect significantly the outcome of the reactions, and in many cases two or three different solid phases were crystallized. A typical reaction for obtaining (K-crypt)₂·tol as one of the crystalline phases starts with 94 mg of K_4Ge_9 dissolved in 1 mL *en* mixed with 216 mg *crypt* (*tol* = toluene, *en* = ethylenediamine, *crypt* = 4,7,13,16,21,24-hexaoxa-1,10-diazabicyclo-[8.8.8]-hexacosane). The resulting brown-red solution is then reacted with 49 mg of SbPh_3 while stirring for 6 h. The solution becomes blood-red. After filtration,

(1) Reviews: (a) Corbett, J. D. *Chem. Rev.* **1985**, *85*, 383. (b) Fässler, T. F. *Coord. Chem. Rev.* **2001**, *215*, 377.

(2) (a) Eichhorn, B. W.; Haushalter, R. C. *J. Am. Chem. Soc.* **1988**, *110*, 8704. (b) Eichhorn, B. W.; Haushalter, R. C. *J. Chem. Soc. Chem. Commun.* **1990**, 937. (c) Gardner, D. R.; Fetting, J. C.; Eichhorn, B. W. *Angew. Chem., Int. Ed. Engl.* **1996**, *35*, 2852 (d) Kesanli, B.; Fetting, J.; Eichhorn, B. *Chem. Eur. J.* **2001**, *7*, 5277. (e) Kesanli, B.; Fetting, J.; Gardner, D.; Eichhorn, B. *J. Am. Chem. Soc.* **2002**, *124*, 4779.

(3) Xu, L.; Sevov, S. C. *J. Am. Chem. Soc.* **1999**, *121*, 9245.

(4) Downie, C.; Tang, Z.; Guloy, A. M. *Angew. Chem., Int. Ed. Engl.* **2000**, *39*, 337.

(5) Ugrinov, A.; Sevov, S. C. *J. Am. Chem. Soc.* **2002**, *124*, 10 990.

(6) Ugrinov, A.; Sevov, S. C. *Inorg. Chem.* **2003**, *42*, 5789.

(7) Ugrinov, A.; Sevov, S. C. *J. Am. Chem. Soc.* **2002**, *124*, 2442.

Table 1. Crystallographic Data for (K-crypt)₂·tol and (K-crypt)₄·3·2.5en.

formula	(K-crypt) ₂ ·tol	(K-crypt) ₄ ·3·2.5en
fw	1929.67	3671.13
space group, Z	<i>P</i> na2 ₁ , 4	<i>P</i> $\bar{1}$, 4
a	23.584(4) Å	14.333(4) Å
b	24.664(4) Å	26.108(8) Å
c	12.910(2) Å	38.64(1) Å
α		80.472(7) °
β		82.169(6) °
γ		84.332(8) °
V	7510(2) Å ³	14085(8) Å ³
ρ_{calc}	1.707 g·cm ⁻³	1.731 g·cm ⁻³
radiation, λ	Mo K α , 0.71073 Å	Mo K α , 0.71073 Å
T	100 K	100 K
μ	40.68 cm ⁻¹	43.33 cm ⁻¹
R1/wR2 (<i>I</i> ≥ 2 σ ₁) ^a	6.46/16.42%	8.40/19.28%
R1/wR2 (all data)	9.66/18.59%	17.34/24.04%

^a R1 = $\sum ||F_o| - |F_c|| / \sum |F_o|$, wR2 = $\{[\sum w[(F_o)^2 - (F_c)^2]^2] / [\sum w(F_o)^2]\}^{1/2}$ for $F_o^2 > 2\sigma(F_o^2)$, w = $[\sigma^2(F_o^2) + (AP)^2]^{-1}$ where $P = [(F_o)^2 + 2(F_c)^2]/3$; A = 0.1 for (K-crypt)₂·tol; A = 0.0891 for (K-crypt)₄·3·2.5en

it is carefully layered with toluene and is then left undisturbed until large enough crystals are formed, 12 days in this case. The mother liquor is decanted and the crystals, orange plates of (K-crypt)₂·tol (yield of up to 55% with respect to Ge) and brown-red polyhedra of (K-crypt)₂Ge₉, are collected. (This latter compound was initially reported as (K-crypt)₂Ge₁₀ but is more likely (K-crypt)₂Ge₉, although the structure has not been properly determined.⁸) A typical reaction for crystallization of (K-crypt)₂·1·en and (K-crypt)₄·3·2.5en starts with 35 mg of K₄Ge₉ and 72 mg *crypt* dissolved in 1 mL *en*. This solution is then reacted with 17 mg SbPh₃ at 65 °C for 4 h while stirring. The resulting red solution is cooled to room temperature, filtered, layered with toluene, and after a few days crystals are recovered. In this case, orange-red plates of (K-crypt)₂·1·en (up to 70% yield), red plates of (K-crypt)₄·3·2.5en (usually 10–15% yield), and brown-red polyhedra of (K-crypt)₂Ge₉ were obtained. Other reactions have produced various combinations of these four compounds and some times also small amounts of (K-crypt)₆Ge₉Ge₉·0.5en with isolated Ge₉³⁻.⁹ It should be pointed out that often the precursor does not dissolve completely, most likely because of presence of impurities, and this limits the control over the amounts of dissolved precursor. Also, these systems are so highly reduced that often manipulations that might be routine for many other systems easily destroy the clusters and result in precipitation of elemental germanium.

¹H NMR spectra of the ethylenediamine solutions before crystallization were taken on a Varian VXR 300 MHz spectrometer (a sealed capillary with C₆D₁₂ + 1% TMS for a reference). They show multiple sets of monosubstituted phenyl rings (6.8–8.0 ppm) due to **1**, **2**, **3**, and various amounts of unreacted SbPh₃ and SbPh₂⁻. This indicates that the three anions are present in all reactions but different sets of them crystallize depending on the specifics of the reaction. In addition, a relatively strong signal of benzene is always observed.

Structure Determination. X-ray diffraction data were collected from an orange plate of (K-crypt)₂·tol (0.23 × 0.17 × 0.02 mm) and a red plate of (K-crypt)₄·3·2.5en (0.18 × 0.12 × 0.02 mm) with graphite-monochromated Mo K α radiation at 100 K on a Bruker APEX diffractometer with a CCD area detector. The structures were solved by direct methods and refined on *F*² using the SHELXTL V5.1 package (after absorption corrections with SADABS). Details of the data collections and refinements are given in Table 1.

Electronic Structure Calculations. Single-point DFT calculations were carried out using the geometry from the structure determination. The Becke 3-parameter density functional with the Lee–Yang–Parr correlation functional (B3LYP)¹⁰ was used in the calculations in

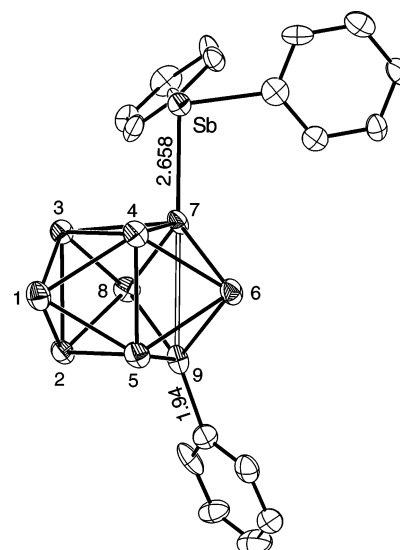


Figure 1. ORTEP drawing (thermal ellipsoids at the 50% probability level) of **2** with the distances [Å] to the two substituents shown. Other important distances are as follows: Ge1–Ge2 2.577(2), Ge1–Ge3 2.606(2), Ge1–Ge4 2.606(2), Ge1–Ge5 2.595(2), Ge2–Ge3 2.705(2), Ge2–Ge5 2.927(2), Ge2–Ge8 2.642(2), Ge2–Ge9 2.602(2), Ge3–Ge4 2.881(2), Ge3–Ge7 2.626(2), Ge3–Ge8 2.643(2), Ge4–Ge5 2.722(2), Ge4–Ge6 2.642(2), Ge4–Ge7 2.634(2), Ge5–Ge6 2.667(2), Ge5–Ge9 2.607(2), Ge6–Ge7 2.572(2), Ge6–Ge9 2.562(2), Ge7–Ge8 2.543(2), Ge7–Ge9 3.098(2), Ge8–Ge9 2.567(2). The angles (deg) at Sb are 93.1(5) for C–Sb–C and 98.2(4) and 96.9(3) for C–Sb–Ge.

conjunction with the 3-21G basis set. The calculations were performed with the Gaussian 98 package, revision A.11.3,¹¹ on Notre Dame’s “Bunch-o-Boxes” Beowulf clusters. Orbital pictures were plotted with Molden.¹² Calculated HOMO–LUMO gaps: 3.04, 3.09, 2.45 eV for **1**, **2**, and **3**, respectively.

Results and Discussion

Structure Description. Crystallographically, there is one type of anion **2** (Figure 1) but two types, **A** and **B**, of anion **3** (Figure 2) in the corresponding structures. However, as it can be seen from Figure 2 as well as based on distances and angles, **A** and **B** are almost identical. The cores of **2** and **3** contain the well-known nine-atom deltahedral clusters of germanium. Such naked clusters have been characterized in numerous compounds, and their geometry and the charge seem to be quite flexible.¹ They can be Ge₉²⁻, Ge₉³⁻, or Ge₉⁴⁻, whereas the geometry is based on a tricapped trigonal prism distorted in various ways and extent. The distortions are always associated with elongation of one, two, or all three edges of the trigonal prism that are parallel to the 3-fold axis. For example, clusters with two elongated edges form the trimers and tetramers of

- (10) (a) Becke, A. D. *Phys. Rev.* **1988**, *38*, 3098. (b) Lee, C.; Yang, W.; Parr, R. G. *Phys Rev B* **1988**, *B37*, 785.
- (11) Gaussian 98, Revision A.11.3. Frisch, M. J.; Trucks, G. W.; Schlegel, H. B.; Scuseria, G. E.; Robb, M. A.; Cheeseman, J. R.; Zakrzewski, V. G.; Montgomery Jr., J. A.; Stratmann, R. E.; Burant, J. C.; Dapprich, S.; Millam, J. M.; Daniels, A. D.; Kudin, K. N.; Strain, M. C.; Farkas, O.; Tomasi, J.; Barone, V.; Cossi, M.; Cammi, R.; Mennucci, B.; Pomelli, C.; Adamo, C.; Clifford, S.; Ochterski, J.; Petersson, G. A.; Ayala, P. Y.; Cui, Q.; Morokuma, K.; Rega, N.; Salvador, P.; Dannenberg, J. J.; Malick, D. K.; Rabuck, A. D.; Raghavachari, K.; Foresman, J. B.; Cioslowski, J.; Ortiz, J. V.; Baboul, A. G.; Stefanov, B. B.; Liu, G.; Liashenko, A.; Piskorz, P.; Komaromi, I.; Gomperts, R.; Martin, R. L.; Fox, D. J.; Keith, T.; Al-Laham, M. A.; Peng, C. Y.; Nanayakkara, A.; Challacombe, M.; Gill, P. M. W.; Johnson, B.; Chen, W.; Wong, M. W.; Andres, J. L.; Gonzalez, C.; Head-Gordon, M.; Replogle, E. S.; Pople, J. A. Gaussian, Inc., Pittsburgh, PA, 2002.
- (12) Schaftenaar, G.; Noordik, J. H. *J. Comput.-Aided Mol. Design* **2000**, *14*, 123.

(8) Belin, C.; Mercier, H.; Angilella, V. *New J. Chem.* **1991**, *15*, 931.

(9) Fässler, T. F.; Schütz, U. *Inorg. Chem.* **1999**, *38*, 1866.

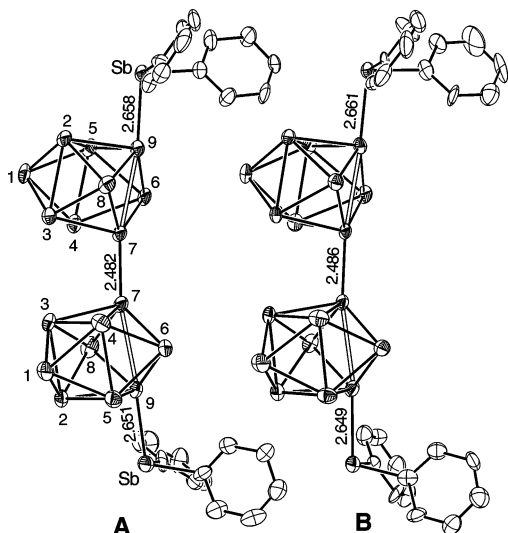


Figure 2. ORTEP drawing (thermal ellipsoids at the 50% probability level) of the two crystallographically different anions **3A** and **3B**.

$[\text{Ge}_9=\text{Ge}_9=\text{Ge}_9]^{6-}$ and $[\text{Ge}_9=\text{Ge}_9=\text{Ge}_9=\text{Ge}_9]^{8-}$, respectively.^{5,6} On the other hand, only one edge is elongated in **1**, **2**, and **3**, the edge 7–9 of the trigonal prism formed by the triangular bases 3–4–7 and 2–5–9 (Figures 1 and 2). This edge in **2** and the pairs of such edges in **3A** and **3B** are 3.098(2), 3.044(2), 3.071(2), 3.054(2), and 3.074(2) Å, respectively, whereas the other two edges, 2–3 and 4–5, are rather normal, 2.705(2) and 2.881(2) Å in **2**, 2.768(2), 2.718(2), 2.726(2), and 2.736(2) Å in **3A**, and 2.765(2), 2.722(2), 2.747(2), and 2.728(2) Å in **3B**. The remaining distances in the clusters are typical for these species and, in general, are longer for atoms with higher coordination.

The substituents, phenyl and diphenylantimony groups, are attached along the elongated edges of the clusters, i.e., to atoms 7 and 9. This is also the case for the intercluster bond in **3** where each Ge_9 cluster acts as a substituent to the other one. The Ge–C distance of 1.94(1) Å in **2** and the average Ge–Sb distance of 2.655 Å in **2** and **3** compare well with similar bonds in other compounds and correspond to single bonds. For example, 1.957(4) Å is the Ge–C distance in Ph_4Ge ,¹³ whereas 2.636 and 2.624 Å are observed for Ge–Sb in $(\text{C}_6\text{H}_5)_3\text{Ge}_2\text{Sb}-\text{Sb}(\text{Ge}(\text{C}_6\text{H}_5)_3)_2$.¹⁴ Also, Ge–Sb distances of 2.6483(5) and 2.6505(5) Å are found in $[\text{Ph}_2\text{Sb}-\text{Ge}_9-\text{SbPh}_2]^{2-}$.⁷ The Ge–Ge distances between the pairs of clusters in **3**, 2.482(2) Å in **3A** and 2.486(2) Å in **3B**, also correspond to a single-bond distance and compare well with the distance of 2.488(1) Å in $[\text{Ge}_9-\text{Ge}_9]^{6-}$ and 2.486(1) Å in $[\text{Ge}_9-\text{Ge}_9]^{8-}$.^{3,4}

Electronic Structure. The observed mode of exo-bonding where the substituents are attached along an elongated edge of the cluster is the only mode observed so far for di-substituted clusters, and the preference seems to originate from the particular shapes of the HOMO and LUMO of the core clusters (below). The same mode of exo-bonding is observed also for **1** and the chains of $[\text{Ge}_9]^{2-}$.^{4,7} Similarly, the single exo-bond for the dimer $[\text{Ge}_9-\text{Ge}_9]^{6-}$ is along the elongated edges of the two clusters.³ Also, the clusters in $[\text{Ge}_9=\text{Ge}_9=\text{Ge}_9]^{6-}$ and $[\text{Ge}_9=\text{Ge}_9=\text{Ge}_9=\text{Ge}_9]^{8-}$ are connected to each other with pairs

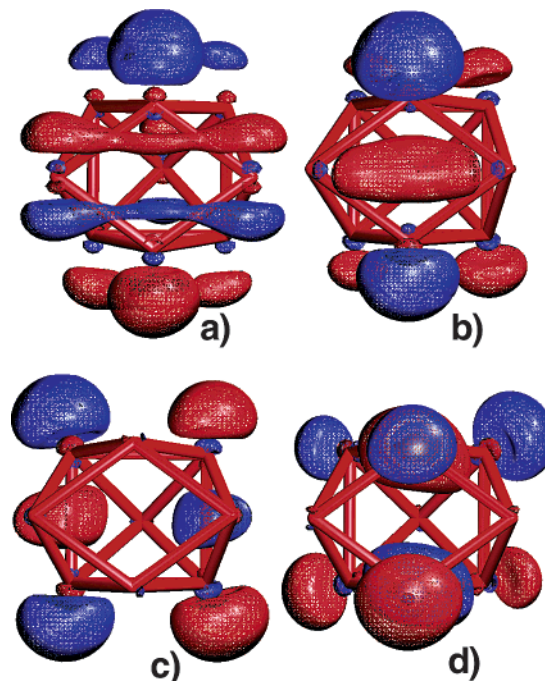


Figure 3. MOLDEN plots of orbitals calculated for the core cluster Ge_9^{2-} in **2**: (a) LUMO, (b) HOMO, (c) HOMO–1, and (d) HOMO–2. The long edge 7–9 (see Figure 1) of the trigonal prism is in front (vertical) and is not drawn.

of bonds that are along the two elongated edges of each cluster.^{5,6} Thus, on the basis of these observations, a more general statement can be made that naked nine-atom clusters always add substituents along the elongated prismatic edges of the clusters. Distinction should be made, however, from various ligated main-group clusters that are directly assembled from atoms that are already bonded to the substituents. For example, the three $\text{Si}(\text{SiMe}_3)_3$ substituents in $[\text{Ge}_9(\text{Si}(\text{SiMe}_3)_3)_3]^-$ are bonded to the three capping atoms of the nine atom cluster with three elongated prismatic edges.¹⁵ However, these species are made by a reaction between $\text{Ge}^{\text{I}}\text{Br}$ and $\text{Li}(\text{Si}(\text{SiMe}_3)_3)_3$ that does not involve preformed Ge_9 clusters.

This specific positioning of the substituents in **1**, **2**, and **3** can be explained with the specifics of the electronic structure of the naked Ge_9 clusters and their ability to carry different charges. DFT calculations on the core nine-atom clusters for all three anions provided very similar results as can be expected from their very similar geometries, and can be generalized for any such cluster with one elongated edge. The LUMO for a charge of 2– (HOMO for Ge_9^{3-} and Ge_9^{4-}) is in a relatively large energy gap, about 2.5 eV from the next higher orbital (LUMO+1) and 1.1 eV from the HOMO, and is quite indifferent of whether it is occupied or not. The calculated energy difference between Ge_9^{4-} and Ge_9^{2-} is only 0.0001 eV. It has been pointed out, some time ago, that this orbital (calculated by the extended-Hückel approach for Bi_9^{5+} with three elongated edges) is almost explicitly composed of the p_z orbitals of the nine atoms (Figure 3a).¹⁶ Also similarly made of p_z orbitals but with almost no participation from the capping atoms are the underlying HOMO and HOMO–1 (Figure 3, parts b and c). Going further down in energy, we find that the next orbital, HOMO–2 (Figure 3d) is made of only $p_x p_y$ of the six atoms forming the prism. The

(13) Karipides, A.; Haller, D. A. *Acta Crystallogr.* **1972**, B28, 2889.

(14) Roller, S.; Dräger, M.; Breunig, H. J.; Ates, M.; Gulec, S. J. *Organomet. Chem.* **1989**, 378, 327.

(15) Schnepf, A. *Angew. Chem., Int. Ed.* **2003**, 42, 2624.

(16) Corbett, J. D.; Rundle, R. E. *Inorg. Chem.* **1964**, 3, 1408.

LUMO is π -bonding within the bases of the prism and σ -bonding to the capping atoms, but it is σ -antibonding between the bases, i.e., along the prismatic edges parallel to z . The HOMO and HOMO-1 (degenerate for ideal D_{3h}), on the other hand, are π -antibonding within the bases but σ -bonding between them, along the prismatic edges. Finally, HOMO-2 is σ -bonding within each base but π -antibonding between them. Therefore, the positions of the LUMO, HOMO, and HOMO-1 will depend very strongly on the number of elongated edges and the extent of the elongation. Larger elongations and a greater number of elongated edges will stabilize the LUMO and destabilize the HOMO and HOMO-1, whereas compression will act in the opposite direction. At the same time, HOMO-2 will be affected very slightly by such distortions along z .

Clearly, both the LUMO and the HOMO are very suitable for interactions with substituents: they are frontier orbitals, both protrude outside the cluster, and both are mostly concentrated at the same two vertexes, those along the long edge. The HOMO is symmetrical while the LUMO is antisymmetrical with respect to the two vertexes of the open edge. These two orbitals, together with the underlying two lone-pair type orbitals at the two vertexes, interact with the corresponding in-phase and out-of-phase combinations of the σ -orbitals of the two substituents. This leads to formation of two strongly bonding, two less bonding, and two antibonding molecular orbitals. The second pair of bonding orbitals are the former LUMO and HOMO of the core cluster being stabilized by the interactions with the substituents. They remain predominantly skeletal bonding orbitals for the cluster but with some mixing from the substituents. This mixing brings them from being the two cluster-bonding orbitals with the highest energy in the naked cluster to the lowest skeletal orbitals in the substituted species. More importantly, these two orbitals, together with HOMO-2 of the naked cluster (Figure 3d), define the positioning of the exo-bonds with respect to the cluster. The two low-lying strongly bonding orbitals that replace the lone pairs involve predominantly germanium s -orbitals and are stereoinactive, i.e., their energies do not depend on the position of the exo-bond. On the other hand, the LUMO and HOMO of the naked cluster point outward along the elongated edge and maximize their overlap when the substituents are positioned along the same direction, i.e., as extensions of the elongated edge. Also, notice that after the stabilization of the former LUMO and HOMO of the naked cluster the orbitals that become frontier are the HOMO-1 and HOMO-2 of the naked cluster. Although HOMO-1 has no contribution from the vertexes of the elongated edge and cannot be stereoactive for the two exo-bonds, HOMO-2 protrudes outside the cluster at these atoms pointing radially with respect to the bases of the prism and will resist bending of these exo-bonds along that direction. Similar sets of orbitals are found for clusters with two elongated edges where two high-lying orbitals are positioned outside these edges and the interactions between such clusters are maximized also along these edges as observed in $[\text{Ge}_9=\text{Ge}_9=\text{Ge}_9]^{6-}$ and $[\text{Ge}_9=\text{Ge}_9=\text{Ge}_9=\text{Ge}_9]^{8-}$.^{5,6} Each cluster in these oligomers participates in the exo-bonding with exactly these two orbitals resulting in a charge of 2^- , independent of whether the cluster is an end or a middle cluster.

The process of replacing two lone pairs (the two antibonding orbitals) with two exo-bonds (the two pairs of bonding orbitals)

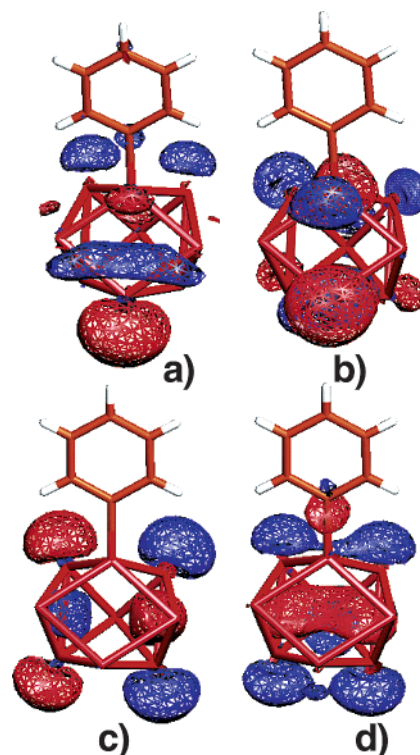


Figure 4. MOLDEN plots of orbitals calculated for hypothetical intermedicate $[\text{Ge}_9\text{-Ph}]^{3-}$ with geometry taken from **2**: (a) HOMO, (b) HOMO-1, (c) HOMO-2, and (d) HOMO-9. The long edge 7-9 (see Figure 1) of the trigonal prism is in front (vertical) and is not drawn.

seems to be directly related to the course of the reaction. To study it in more detail, calculations were carried out also on the cluster with one substituent, the phenyl group (chosen over SbPh_2 for the simpler drawings; the results with SbPh_2 are identical). Shown in Figure 4 are the HOMO, HOMO-1, HOMO-2, and HOMO-9 of such a hypothetical monosubstituted cluster, $[\text{Ge}_9\text{-Ph}]^{3-}$. Clearly, the phenyl group has stabilized the HOMO of the naked Ge_9^{2-} cluster (Figure 3b) lowering its energy to HOMO-9 (Figure 4d). Nevertheless, this orbital remains predominantly skeletal for the cluster as most of it is distributed over the cluster. There is another, much lower-lying orbital that is predominantly responsible for the exo-bond (not shown). Notice that the HOMO of $[\text{Ge}_9\text{-Ph}]^{3-}$ (Figure 4a) originates from the LUMO of Ge_9^{2-} (Figure 3a). It is somewhat perturbed, of course, by the interactions with the phenyl group, but is still concentrated outside the second vertex of the elongated edge (bottom) and is still along the same direction as in the naked cluster. Furthermore, exactly as the LUMO of the naked Ge_9^{2-} cluster (Figure 3a), this orbital is in a large energy gap, 1.98 eV from the next higher orbital and 1.06 eV from the one below it. (It is the LUMO for $[\text{Ge}_9\text{-Ph}]^-$.) Also, similarly to Ge_9^{4-} and Ge_9^{2-} , the energy difference between the species with occupied and empty orbital, $[\text{Ge}_9\text{-Ph}]^{3-}$ and $[\text{Ge}_9\text{-Ph}]^-$, respectively, is only 5.8×10^{-5} eV (0.00188 eV for $[\text{Ge}_9\text{-SbPh}_2]^{3-}$ and $[\text{Ge}_9\text{-SbPh}_2]^-$). Thus, in analogy with the existence of nine-atom clusters of germanium with different charges, Ge_9^{4-} , Ge_9^{3-} , and Ge_9^{2-} , it is very likely that species such as $[\text{Ge}_9\text{-Ph}]^{3-}$, $[\text{Ge}_9\text{-Ph}]^{2-}$, and $[\text{Ge}_9\text{-Ph}]^-$ can exist as well. This orbital, the HOMO of $[\text{Ge}_9\text{-Ph}]^{3-}$, in the disubstituted species is also stabilized, and the top two orbitals are the HOMO-1 and HOMO-2 of $[\text{Ge}_9\text{-Ph}]^{3-}$ (Figures 4b and 4c). Again, whereas HOMO-2 has no contribution from

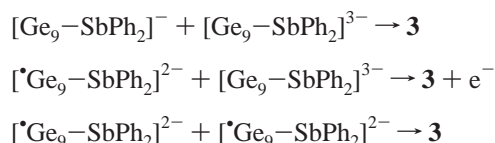
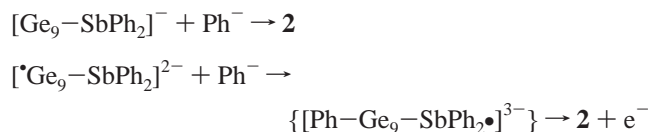
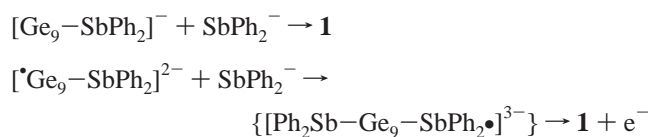
the exo-bonded vertexes, HOMO–1 does and plays stereoactive role for the positioning of the exo-bonds.

Reaction Description. The addition of various groups to the Ge_9 cluster can be described as a replacement of a lone pair of electrons at a germanium vertex by an exo-bond between the substituent and that vertex. The course of the reaction is most likely very similar to $\text{S}_{\text{N}}1$ and/or $\text{S}_{\text{RN}}1$ nucleophilic substitutions where the nucleophiles, SbPh_2^- and Ph^- in our case, interact with an empty or half-filled orbital of the substrate. The difference with the classical mechanisms is that the leaving group is one or more electrons. Similarly to the classical mechanisms this step results in an empty or half-filled low-lying orbital available for the nucleophilic attack. Another difference is that the leaving electrons in our case are also the electrons that reduce SbPh_3 and generate the nucleophiles SbPh_2^- and Ph^- . In classical reactions the nucleophiles are often generated by separate reduction with alkali metals.

The “release” of electrons by the clusters needs some more elaboration and discussion. We have proposed in the past that Ge_9 clusters with different charges, i.e., Ge_9^{4-} , Ge_9^{3-} , and Ge_9^{2-} , coexist in the ethylenediamine solutions, and that depending on the available countercations different species crystallize. We have now carried out two experiments that prove this very convincingly. First, a saturated dark brown-green solution of K_4Ge_9 was divided equally in four test tubes labeled from #1 to #4. Added to these four containers were the following reagents (molar ratio to potassium is in parentheses): #1, crypt (1.5:1); #2, crypt (0.3:1); #3, 18-crown-6 ether (1:1) and heated at 50 °C for 2 h; and #4, nothing. They were all then layered carefully with toluene except that the toluene for test tube #4 was saturated with 18-crown-6 ether. After a few days, various compounds crystallized from these test tubes: #1, (K-crypt) $_6$ (Ge_9)(Ge_9) $\cdot 0.5\text{en}$ with monomers of Ge_9^{3-} ; #2, both (K-crypt) $_6$ (Ge_9)(Ge_9) $\cdot 0.5\text{en}^9$ and (K-crypt) $_2\text{K}_4$ [Ge_9 – Ge_9] $\cdot 8\text{en}$ with dimers of [Ge_9 – Ge_9] $^{6-}$; #3, (K-18C6) $_6$ [Ge_9 – Ge_9] $\cdot 2\text{en}$ with trimers of [Ge_9 – Ge_9 – Ge_9] $^{6-}$; #4, both (K-18C6) $_2\text{K}_2\text{Ge}_9$ with monomers of Ge_9^{4-} and (K-18C6) $_3\text{Ge}_9$ $\cdot 3\text{en}$ with monomers of Ge_9^{3-} .¹⁷ Thus, these compounds contain nine-atom clusters with different charges: Ge_9^{4-} as monomers, Ge_9^{2-} in the trimer, and Ge_9^{3-} as monomers and in the dimer. The second experiment is even more telling. A saturated dark red-brown solution of Rb_4Ge_9 in ethylenediamine was prepared. Added to this solution were both crypt and 18-crown-6 ether, each in a molar ratio of 2:1 with respect to Ge_9 . After layering with toluene and waiting for a few days, the following phases were found in the solid product: (Rb-crypt) $_6$ [Ge_9 – Ge_9 – Ge_9] $\cdot 3\text{en}$,⁵ (Rb-18C6) $_8$ [Ge_9 – Ge_9 – Ge_9] $\cdot 2\text{en}$,⁶ (Rb-crypt) $_2\text{Rb}_4$ (Ge_9)(Ge_9) $\cdot 7\text{en}$,¹⁷ and (Rb-18C6) $_2\text{Rb}_2\text{Ge}_9$.¹⁷ Thus, nine-atom clusters with all three charges can cocrystallize from the same solution.

How is it possible that Ge_9^{4-} , Ge_9^{3-} , and Ge_9^{2-} coexist in these solutions? Most likely there are equilibria between themselves and free electrons, i.e., $\text{Ge}_9^{4-} \rightleftharpoons \text{Ge}_9^{3-} + \text{e}^-$ and $\text{Ge}_9^{3-} \rightleftharpoons \text{Ge}_9^{2-} + \text{e}^-$. This is exactly the same phenomenon as observed for elemental alkali metals when dissolved in ethylenediamine or liquid ammonia, $\text{A} \rightleftharpoons \text{A}^+ + \text{e}^-$ (A = alkali

metal).¹⁸ The free electrons are solvated by the ethylenediamine and, although they react with the solvent to produce amide and hydrogen, the reaction is very slow in the absence of catalysts or strong nucleophiles.¹⁸ These electrons, however, react readily with SbPh_3 to produce nucleophiles, Ph^- and initially a radical of *SbPh_2 which becomes SbPh_2^- . This is exactly the same reaction as the well-known generation of nucleophiles using elemental alkali metals dissolved in liquid ammonia, i.e., $2\text{A} + \text{SbPh}_3 \rightarrow 2\text{A}^+ + \text{SbPh}_2^- + \text{Ph}^-$. The phenyl anion is quite reactive and extracts a proton from the ethylenediamine to form benzene and amide. The presence of large amounts of benzene was confirmed by proton NMR in all of the reactions. Due to the simultaneous presence of numerous differently bonded phenyl groups it was impossible to unequivocally assign a set of phenyl hydrogens in the ^1H NMR to the other nucleophile, SbPh_2^- . However, the existence of the nucleophile SnPh_3^- was shown by ^{119}Sn -NMR (Bruker 400 MHz, a sealed capillary with C_6D_{12} as a reference, Me_4Sn in pyridine as an external reference) in similar reactions of Ge_9 clusters with SnPh_4 in pyridine. The anion coexists with the corresponding triphenyltin-substituted germanium clusters.¹⁹ More importantly, triphenyltin substituted clusters were later obtained also from reactions of K_4Ge_9 with the preformed nucleophile Ph_3Sn^- prepared by reduction of Ph_3SnCl with potassium metal. Thus, it is clear that all of these addition reactions, either with tin- or antimony-based compounds, start with the nucleophile donating electrons to the LUMO of Ge_9^{2-} ($\text{S}_{\text{N}}1$ -like), $\text{Ge}_9^{2-} + \text{SbPh}_2^- \rightarrow [\text{Ge}_9\text{–SbPh}_2]^{3-}$, or to the half-occupied HOMO of the radical *Ge_9^{3-} ($\text{S}_{\text{RN}}1$ -like), $\text{*Ge}_9^{3-} + \text{SbPh}_2^- \rightarrow \{[\text{*Ge}_9\text{–SbPh}_2]^{4-}\} \rightarrow [\text{Ge}_9\text{–SbPh}_2]^{3-} + \text{e}^-$. The resulting monosubstituted species, either $[\text{Ge}_9\text{–SbPh}_2]^{3-}$ or $[\text{Ge}_9\text{–Ph}]^{3-}$, have not been isolated yet but should be relatively stable. As already discussed, their HOMOs are of exactly the same type as the HOMO of Ge_9^{4-} (Figure 3a), which is the LUMO of Ge_9^{2-} . Their character is also the same, i.e., they are in large energy gaps and there is very small energy differences between when occupied and empty. Thus, we propose that monosubstituted species of different charges exist in the solutions and they form equilibria similar to the naked clusters, i.e., $[\text{Ge}_9\text{–SbPh}_2]^{3-} \rightleftharpoons [\text{*Ge}_9\text{–SbPh}_2]^{2-} + \text{e}^-$ and $[\text{*Ge}_9\text{–SbPh}_2]^{2-} \rightleftharpoons [\text{Ge}_9\text{–SbPh}_2]^{-} + \text{e}^-$. The final products are formed when another nucleophile attacks the empty LUMO of $[\text{Ge}_9\text{–SbPh}_2]^{-}$ or the half-occupied HOMO of $[\text{*Ge}_9\text{–SbPh}_2]^{2-}$ as follows:



These multiple possibilities for reactions of different species with different nucleophiles are clearly manifested in the mul-

(17) For structure details see the CIF file in Supporting Information: (K-crypt) $_2\text{K}_4$ [Ge_9 – Ge_9] $\cdot 8\text{en}$ contains the same dimers of [Ge_9 – Ge_9] $^{6-}$ as those reported for (K-crypt) $_2\text{Cs}_4$ [Ge_9 – Ge_9] $\cdot 6\text{en}$.³ (K-18C6) $_6$ [Ge_9 – Ge_9 – Ge_9] $\cdot 2\text{en}$ contains the same trimers of [Ge_9 – Ge_9 – Ge_9] $^{6-}$ as those reported for (Rb-crypt) $_6$ [Ge_9 – Ge_9 – Ge_9] $\cdot 3\text{en}$.⁵ (K-18C6) $_2\text{K}_2\text{Ge}_9$ and (Rb-18C6) $_2\text{Rb}_2\text{Ge}_9$ are isostructural and contain isolated Ge_9^{4-} clusters. (K-18C6) $_3\text{Ge}_9$ $\cdot 3\text{en}$ and (Rb-crypt) $_2\text{Rb}_4$ (Ge_9)(Ge_9) $\cdot 7\text{en}$ contain isolated Ge_9^{3-} clusters.

tiphase crystalline products obtained from such reactions. It is possible that other anions form as well but cannot be crystallized with the available counteranions. Thus, species such as $[\text{Ph}-\text{Ge}_9-\text{Ph}]^{2-}$, $[\text{Ph}-\text{Ge}_9-\text{Ge}_9-\text{SbPh}_2]^{4-}$, $[\text{Ph}-\text{Ge}_9-\text{Ge}_9-\text{Ph}]^{4-}$, etc., should not be ruled out. Also, as mentioned in the experimental part, often found in the product are the naked Ge_9^{3-} and Ge_9^{2-} coexisting with **1**, **2**, and/or **3**. This clearly indicates that not only Ph^- undergoes side reactions but perhaps SbPh_2^- does that as well. Furthermore, anion **1** exists also with bismuth, i.e., $[\text{Ph}_2\text{Bi}-\text{Ge}_9-\text{BiPh}_2]^{2-}$, and perhaps **2** and **3** are possible. However, none of the corresponding arsenic and phosphorus analogues of these species has been made. The analogous reactions with AsPh_3 and PPh_3 result in the more oxidized clusters of Ge_9^{2-} found as oligomers ($[\text{Ge}_9=\text{Ge}_9=\text{Ge}_9]^{6-}$ or $[\text{Ge}_9=\text{Ge}_9=\text{Ge}_9=\text{Ge}_9]^{8-}$) and the corresponding free nucleophiles AsPh_2^- and PPh_2^- . It is possible that phenyldisubstituted species are formed but, as in the reactions with SbPh_3 and BiPh_3 , they do not crystallize. The failure to synthesize phosphorus and arsenic analogues of **1**, **2**, and/or **3**, is most likely due to the less nucleophilic nature of the corresponding anions PPh_2^- and AsPh_2^- .

- (18) Kraus, C. A. *J. Am. Chem. Soc.* **1908**, *30*, 1323. (b) Thompson, J. C. *Electrons in Liquid Ammonia*; Clarendon Press: Oxford, 1976.
- (19) ^{119}Sn -NMR of pure $[\text{Ph}_3\text{Sn}-\text{Ge}_9-\text{SnPh}_3]^{2-}$ in pyridine (Bruker 400 MHz, a sealed capillary with C_6D_{12} as a reference, Me_4Sn in pyridine as an external reference): -108.1 ppm for Ph_3Sn^- and 15.1 ppm for $[\text{Ph}_3\text{Sn}-\text{Ge}_9-\text{SnPh}_3]^{2-}$. ^{119}Sn -NMR of Ph_3SnCl reacted with K in ethylenediamine (Bruker 400 MHz, a sealed capillary with C_6D_{12} as a reference, Me_4Sn in CHCl_3 as an external reference): -113.12 ppm for Ph_3Sn^- (the shift of 5 ppm is due to the different solvent).

Summary

The reaction between Ge_9^{n-} where $n = 2, 3$, or 4 , and SbPh_3 produces $[\text{Ph}_2\text{Sb}-\text{Ge}_9-\text{SbPh}_2]^{2-}$, $[\text{Ph}-\text{Ge}_9-\text{SbPh}_2]^{2-}$, $[\text{Ph}_2\text{Sb}-\text{Ge}_9-\text{Ge}_9-\text{SbPh}_2]^{4-}$, and perhaps other species that have not been characterized yet. The reaction proceeds via formation of negatively charged nucleophiles Ph^- and SbPh_2^- from SbPh_3 and the solvated free electrons that are released from the nine-atom clusters. High-energy cluster orbitals with significant distribution outside the cluster are available for the nucleophilic attack and formation of bonds. Different products are formed depending upon the available nucleophile in the immediate vicinity of the cluster. This knowledge can be used to envision other, more interesting cluster-based species.

Acknowledgment. We thank the National Science Foundation (CHE-0098004) and the Petroleum Research Fund (37301-AC5,3), administered by the ACS, for the financial support of this research, Iliya Todorov for synthesis of the precursors, and Di-Fei Wang for help with the DFT calculations. The “Bunch-o-Boxes” cluster was built with the financial assistance of the NSF Major Research Initiative program (DMR-0079647).

Supporting Information Available: X-ray crystallographic file in CIF format (7 structures) is available free of charge via the Internet at <http://pubs.acs.org>.

JA037007B